Analysis of the influence of fluid saturation on elastic velocities of sandstones and carbonates using laboratory methods and fluid substitution models

Leyllanne Renalle Batista de Almeida[1], José Agnelo Soares[1], Pedro Henrique Alves de Lima[1].
[1]Laboratório de Petrofísica, Universidade Federal de Campina Grande

This paper was prepared for presentation during the 15th International Congress of the Brazilian Geophysical Society held in Rio de Janeiro, Brazil, 31 July to 3 August, 2017.

Abstract

The influence of fluid saturation on compressional and shear velocities is an important issue to be solved by geophysicists in order to provide better efficiency for seismic monitoring of reservoirs. It is extremely important to carry out the analysis of the physical properties of rocks under different saturation conditions. In this context, fluid substitution models are the basis for 4D seismic monitoring, from which they can quantify and model the most different production scenarios. In this research, the influence of fluid saturation on elastic wave velocities was observed for sandstone, limestone and dolomite samples. Results combined laboratorial experiments (rock physics) and empirical methods (fluid substitution models). Gassmann and Brown & Korringa models estimated the same values of wave velocities for carbonate rocks due to its homogeneous mineralogical composition. Although sandstone samples are heterogeneous there are not a strong influence of heterogeneity on wave velocities according to Brown & Korringa model, making it less efficient. Gassmann and Brown & Korringa models were more efficient to estimate the compressional wave velocities, while the Biot model made better predictions of shear wave velocities.

Introduction

Hydrocarbons are stored in reservoir rocks, which may be sandstones or carbonates. These rocks are usually a cluster of minerals, and may contain organic matter in their composition, which often occurs in carbonates (Almeida, 2017). In this context, rock physics provides the basis of seismic monitoring for such reservoirs and connections for seismology, geology and engineering applications, transforming seismic properties into reservoir parameters. In addition, these properties should be well understood for direct detection of hydrocarbons and also for the post-prospection, with the monitoring of fluid flow through the reservoir, known as 4D seismic (Wang e Nur, 2000). In order to improve quantitative results of 4D seismic it is necessary to establish the theoretical relationship between the seismic attributes and the petrophysical characteristics of the reservoir (Griscenco, 2015).

Fluids found in sedimentary rocks can vary greatly in composition and physical properties, causing variations on seismic properties. Therefore, it is extremely important to study rocks under different conditions of saturation. However there is a limitation on the performance of studies in active production reservoirs, since it is not possible to perform direct analysis on reservoir rocks from fields in production. Provided the difficulty of analyzing such samples, analogous onshore occurrences are studied. Petrophysical characterization is performed on samples from outcrops, which enables the elaboration of geological models from petrophysical properties databases. The study of analogues promotes determination of the spatial distribution of petrophysical properties controlling accumulations of hydrocarbons in a scale of detail often not obtained through the seismic interpretation (Sousa, 2005). Acoustic properties are affected by the presence of fluids, mainly in two ways: change in the elastic modulus of the rock and its seismic response, and by the introduction of velocity dispersion, which is the variation of velocity with frequency (Sengupta, 2000).

Through laboratory methods, conditions of subsurface can be reproduced approaching the real conditions to which the rocks are submitted. Lab-measured elastic wave velocities were acquired under different levels of confining stress. On the other hand, there are some theoretical models to obtain elastic constants and elastic velocities of saturated rocks which use properties of dry rocks as input data. Such models are widely applied and known as fluid substitution models. Some of these models are Gassmann (1951), Biot (1956a, 1956b, 1962) and Brown & Korringa (1975). Gassmann's equation (1951) is the most used to calculate variations of seismic properties on rocks with different fluid saturations in the reservoir. However, although these models still present limitations with respect to the complexity and anisotropy of rocks. Due to these limitations, Brown & Korringa (1975) generalized the Gassmann equation for heterogeneous and anisotropic media. While Gassmann model is used for low frequency waves, a reason for caution, since laboratory tests the rocks are subjected to the propagation of waves at high frequencies, Biot (1956, 1962) developed a mathematical model for seismic and ultrasonic measurements in high frequency (Trovão, 2015).

This paper provides the study of sedimentary rocks (sandstones and carbonates) from US outcrops. Table 1 shows the lithology, the nomenclature of samples and geographic location of outcrops from which they were extracted.

The objective of this research is to analyze the influence of fluid saturation on dynamic elastic properties of sandstones and carbonate rocks, using laboratory methods and application of theoretical fluid substitution models. The models of Gassmann (1951), Biot (1962) and Brown & Korringa (1975) are used**.**

Table 1: Litology, sample nomenclature and geographical location.

Litology	Sample	Geographical location
Sandstone	CGS-015	Colorado
Sandstone	PSS-002	Texas
Sandstone	SCS-001	Ohio
Limestone	IL3-020	Indiana
Limestone	AC-012	Texas
Dolostone	SD-12	Illinois

Method

Sedimentary rock plugs of approximately 50 mm in length and 38 mm in diameter were prepared. Figure 1 shows the plugs studied.

Figure 1: Samples studied.

Initially density and porosity tests were performed, since this information is necessary to compute elastodynamic results for the dry samples. Experiments were conducted using the AutoLab 500® system, which allows the simultaneous record of three waveforms: P-wave, which propagates and has polarization in the axial direction of the plug, and two S-waves with mutually orthogonal polarization directions perpendicular to the axis of the plug, named S_1 and S_2. During the first measurements, performed for dry samples, pore pressure and temperature were kept under room conditions and wave velocities are recorded for decreasing intervals of confining pressure starting from 35 MPa. After the first wave was captured, the pressure is decreased and the other waves are captured with confining pressures less than the first (30, 25, 20, 15, 10, 5) MPa. Then the wave picking is performed, which is the marking of the arrival time of each of these waves. Afterwards samples were saturated with deionized water and mineral oil separately and the same tests were performed. The procedure was similar, however, the pore system was used to keep saturation. Fluids were injected at 5MPa of pore pressure and the initial confining pressure of the system was 40MPa.

Succeeding elastic wave measurements, a sub-sample was extracted from analyzed plugs (Figure 2), for acquisition of X-ray microtomography images. From these images, using Avizo Fire software, it is possible to obtain the required tortuosity factor to predict the elastic properties using the Biot model.

Figure 2: Preparation of a sub-sample for the acquisition of CT scans.

Subsamples were sent to the Laboratory of porous media and thermophysical properties of the Federal University of Santa Catarina. The microtomographic images were acquired by the XRADIA equipment, model Versa XRM 500, images of very high resolution around 2.4 μm for the samples studied. The microtomographic images were used for generation of 3D computational models with segmentation of the constituent phases in Avizo Fire software. The analysis is based on the grey scale level of each phase, being able to vary from level zero (less dense), to level 255 (more dense).

After subvolume segmentation, using the previously obtained thresholds, a single tool was applied to the generated result, which was Centroid Path Tortuosity. From this point on, the tortuosity factor was obtained. Figure 3 shows the flowchart with the procedures used to obtain this factor.

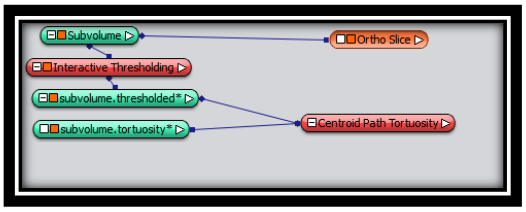

Figure 3: Work flow diagram used to acquire tortuosity.

For Brown & Korringa model, it was necessary to acquire the mineralogical composition of the rocks. For the compositional analysis, discs were also extracted from the plugs studied, to prepare the samples sent to the XRD analysis. These analysis were carried out by the Regional Center for Technological Development and Innovation of the Federal University of Goiás (CRTI) and by the Petrobras Research Center (CENPES).

Gassmann model assumes several assumptions which in most non-conventional reservoirs are not satisfied, such as isotropy and homogeneity. To obtain the incompressibility Equation (1) is used.

$$\frac{Ksat}{Kmin-Ksat} = \frac{\text{Kdry}}{Kmim-Kdry} + \frac{K_{fl}}{\phi(K_{min}-\text{K}_{fl})}; G_{sat} = G_{dry} \qquad (1)$$

Where,

Ksat- Incompressibility of saturated rock;
Kmin- Mineral incompressibility;
Kdry- Dry rock incompressibility;
Kfl- Incompressibility of the saturating fluid;
Ø- Porosity of the rock;
Gsat- Shear modulus in saturated rock e
Gdry- Dry rock shear modulus.

After calculating incompressibility of the saturated rock by the Gassmann model, compressional and shear wave velocities for saturated rock are calculated with the aid of the average saturated rock density (Equations 2 and 3).

$$V_{psat} = \frac{\sqrt{\mathrm{k}_{sat} + \frac{4}{3} G_{sat}}}{\rho_{sat}} \quad (2)$$

$$V_{ssat} = \sqrt{\frac{G_{sat}}{\rho_{sat}}} \quad (3)$$

For high frequencies the model used is the Biot model (1962). In this model velocities for high frequencies were obtained by equations (4) to (13).

$$Vp\infty = \frac{\{\Delta + [\Delta^2 - 4(\rho_{11}\rho_{22} - \rho^2{}_{12})(\mathrm{PR} - Q^2)]^{1/2}}{2(\rho_{11}\rho_{22} - \rho_{12}{}^2)} \quad (4)$$

$$Vs_\infty = \frac{G_{dry}}{\rho - \phi\rho_{fl}\alpha^{-1}} \quad (5)$$

$$\Delta = P\rho_{22} + R\rho_{11} - 2Q\rho_{12} \quad (6)$$

$$P = \frac{(1-\phi)\left(1-\phi\frac{K_{dry}}{K_{min}}\right)K_{min} + \phi\frac{K_{min}K_{dry}}{K_{fl}}}{1-\phi\frac{K_{dry}}{K_{min}} + \phi\frac{K_{min}}{K_{fl}}} + \frac{4}{3}G_{dry} \quad (7)$$

$$Q = \frac{\left(1-\phi\frac{K_{dry}}{K_{min}}\right)\phi K_{min}}{1-\phi\frac{K_{dry}}{K_{min}} + \phi\frac{K_{min}}{K_{fl}}} \quad (8)$$

$$R = \frac{\phi^2 K_{min}}{1-\phi\frac{K_{dry}}{K_{min}} + \phi\frac{K_{min}}{K_{fl}}} \quad (9)$$

$$\rho_{11} = (1-\phi)\rho_{min} - (1-\alpha)\phi\rho_{fl} \quad (10)$$

$$\rho_{22} = \alpha\phi\rho_{fl} \quad (11)$$

$$\rho_{12} = (1-\alpha)\phi\rho_{fl} \quad (12)$$

$$\rho = \rho_{min}(1-\phi) + \rho_{fl}\phi \quad (13)$$

The Biot velocities for compressional and shear waves are Vp∞ and Vs∞, G is the shear modulus of the rock, Kdry, Kfl and Kmin, respectively are the incompressibility modules of dry rock, fluid and rock mineral matrix, Ø is the porosity, ρ, ρmin and ρfl are respectively the mean densities of the saturated rock, the rock mineral and the saturating fluid, α is the tortuosity factor of the rock channels. Density variations due to the relative movement between pore and fluid in the rock matrix, rock / pore system and saturating fluid are represented by ρ11, ρ12, ρ22. For fully rectilinear and parallel channels, α is equal to 1, and for the totally random channel system, α is equal to 3.

Brown and Korringa (1975) estimate the incompressibility and shear modulus for heterogeneous and anisotropic rocks. The principle is a generalization of the Gassmann equation (1951) as a function of incompressibility modules of the solid phase and incompressibility module of the porous phase (Equation 14). For the calculation of velocities, the same equations are used of Gassmann (Equations 2 and 3).

$$\frac{K_{sat}}{K_s - K_{sat}} = \frac{K_{dry}}{K_s - K_{dry}} + \frac{K_{\phi s}}{K_s}\frac{K_{fl}}{[\phi(K_\phi - K_{fl})]} \quad (14)$$

Where,

Kdry- Dry rock incompressibility;
Ksat- Incompressibility of saturated rock;
KØs- Pore incompressibility;
Kfl- Incompressibility of the saturating fluid,
Ø- Porosity of the rock.

Results

From figures 4 to 15, it is generally observed that for most of the samples there is a small variation of the compressional wave velocity with the decrease of the effective pressure, both for the values obtained conventionally, and in the estimated velocities through the fluid replacement models. In contrast, there is a considerable drop in the shear wave velocity with the decrease of this pressure.

For samples of carbonate rocks (Figures 4 to 9), the Gassmann and Brown & Korringa models estimate the same velocity values. This is due to the fact that the composition of these samples is homogeneous, so the Brown & Korringa model, which takes into account the heterogeneity of the rock, is reduced to the Gassmann model, whose premise is that they are homogeneous. The rocks of sandstone matrix have a heterogeneous and variable composition. Thus, we can see in figures 10 to 15 an additional curve, related to the Brown & Korringa model.

Biot model requires tortuosity factor data to calculate the velocity. This property was obtained from the analysis of computational plugs through X-ray microtomography images. For the samples studied, it was observed that the compressional wave velocity estimated by this model remained lower than the other methods.

For the samples of sandstone matrix studied, the values of laboratory velocity are higher than or equal to the empirical models, for the compressional and shear waves, except for the Vs of the PSS-02 sample saturated with water (Figure 12). Gassmann and Brown & Korringa models have come close to each other and also to the conventional method.

Biot model presented the lowest velocity values for the compressional waves and values close to the other models for the shear waves. Still for these waves, Gassmann and Brown & Korringa models presented the same velocities, both for the water saturated samples and for the oil saturated samples.

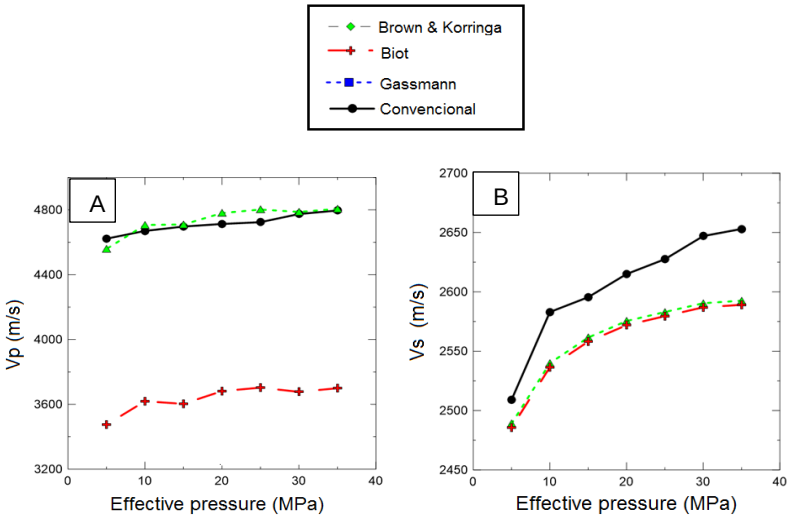

Figure 4: Relation between compressional and shear velocities with pressures for limestone IL3-20: (A) and (B) saturated with water.

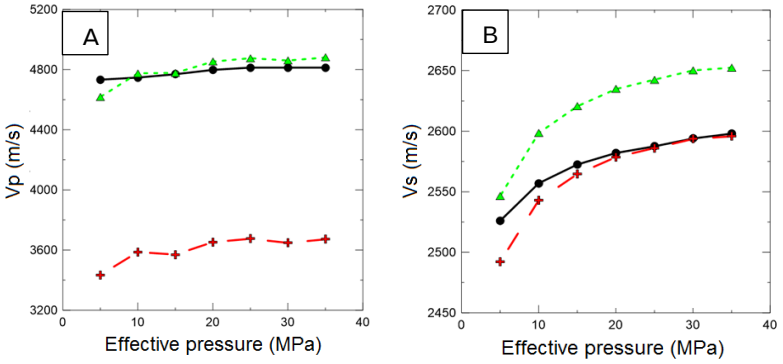

Figure 5: Relation between compressional and shear velocities with pressures for limestone IL3-20: (A) and (B) saturated with oil.

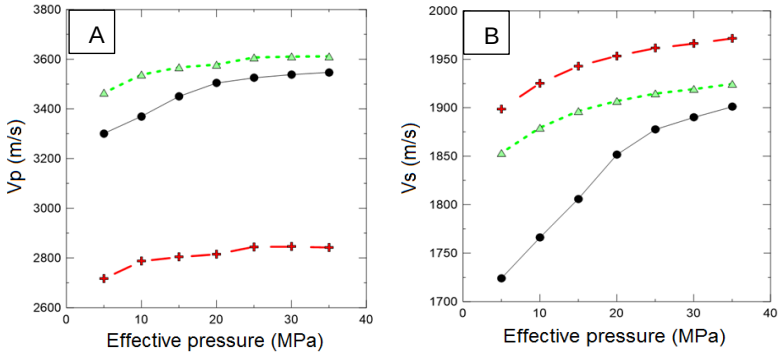

Figure 6: Relation between compressional and shear velocities with pressures for limestone AC-12: (A) and (B) saturated with water.

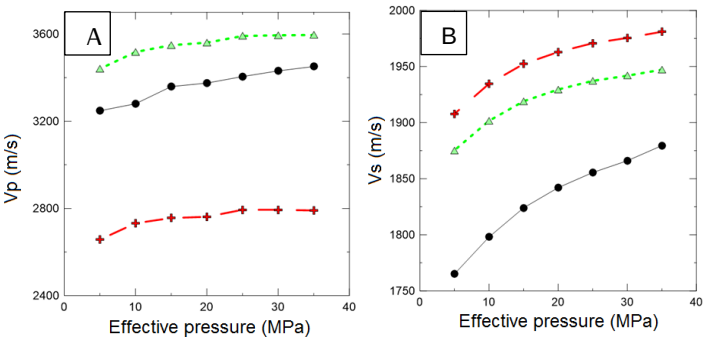

Figure 7: Relation between compressional and shear velocities with pressures for limestone AC-12: (A) and (B) saturated with oil.

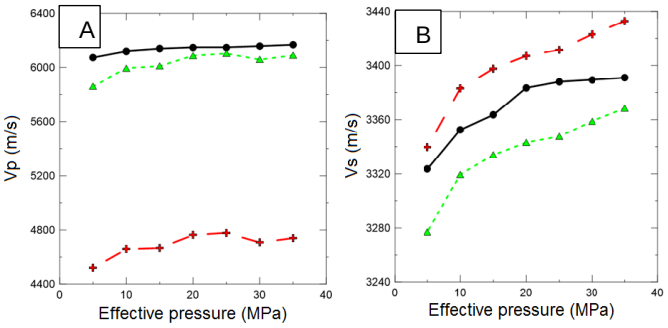

Figure 8: Relation between compressional and shear velocities with pressures for limestone SD-12: (A) and (B) saturated with water**.**

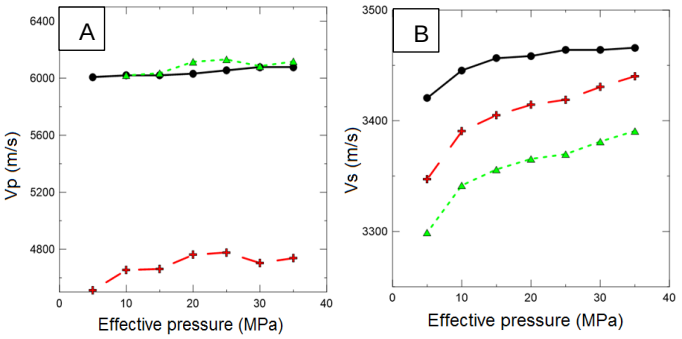

Figure 9: Relation between compressional and shear velocities with pressures for limestone SD-12: (A) and (B) saturated with oil**.**

As already mentioned, when the rock samples are heterogeneous the models of Gassmann and Brown & Korringa are distinguished, as was the case of the sandstones studied. Analyzing the results obtained for the two models, a small variation of the P-wave velocity was observed. For the more homogeneous sample (PSS-02), the velocity value remained practically unchanged between the two models, as expected. For the other samples, despite the small variation, the velocities obtained by the Brown & Korringa model were higher than those obtained by the Gassmann model, for the CGS-015, and lower for the SCS-01.

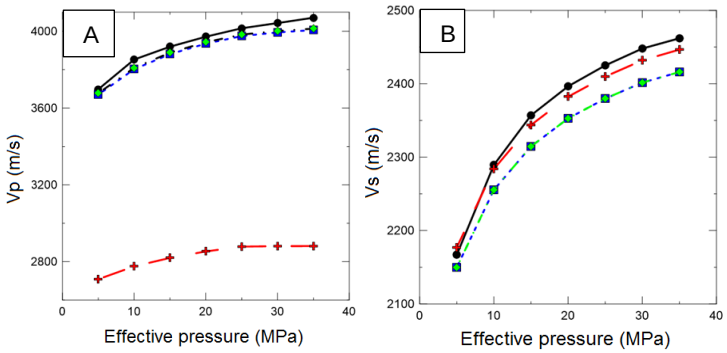

Figure 10: Relation between compressional and shear velocities with pressures for limestone SCS-01: (A) and (B) saturated with water**.**

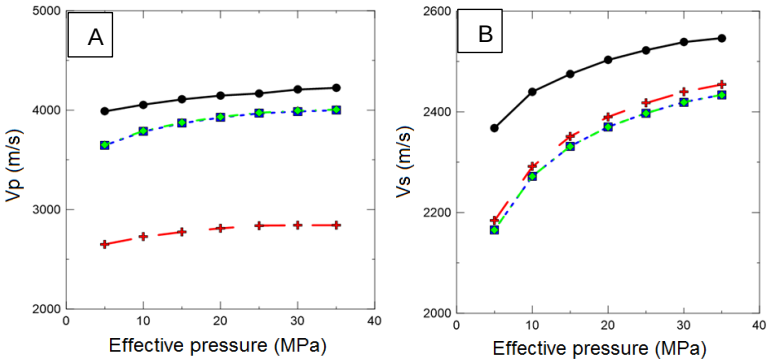

Figure 11: Relation between compressional and shear velocities with pressures for limestone SCS-01: (A) and (B) saturated with oil**.**

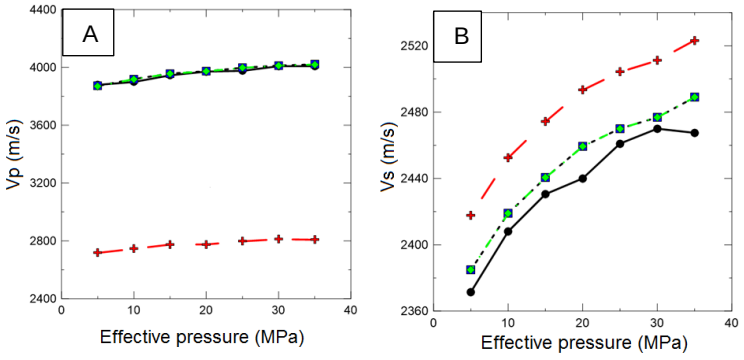

Figure 12: Relation between compressional and shear velocities with pressures for limestone PSS-02: (A) and (B) saturated with water**.**

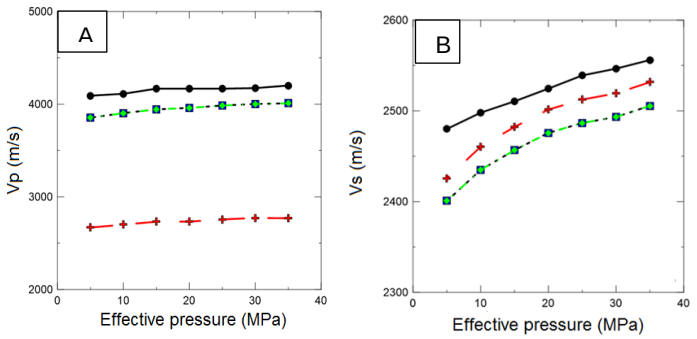

Figure 13: Relation between compressional and shear velocities with pressures for limestone PSS-02: (A) and (B) saturated with oil.

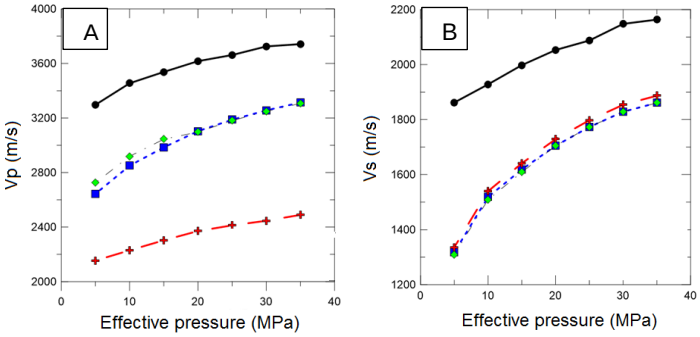

Figure 14: Relation between compressional and shear velocities with pressures for limestone CGS-015: (A) and (B) saturated with water**.**

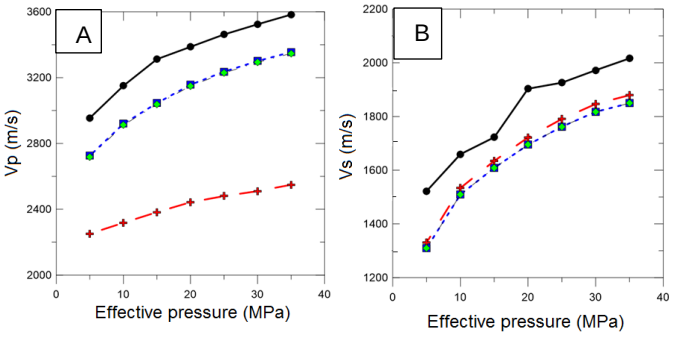

Figure 15: Relation between compressional and shear velocities with pressures for limestone CGS-015: (A) and (B) saturated with oil**.**

Conclusions

For the samples of carbonates rocks used in this research, the Gassmann and Brown & Korringa models estimate the same velocity values due to their homogeneity. However, for sandstones, the Brown & Korringa model presents a small variation in velocity in relation to the Gassmann model, due to the heterogeneous composition of these rocks. But it showed little efficiency.

Gassmann and Brown & Korringa models were more effective for the compressional wave velocities and in some cases also fitted

well for the shear waves. Biot has adjusted better for the shear waves, especially for sandstones.

References

ALMEIDA, L. R. B. (2017) . **Análise petrofísica e petrográfica de padrões internacionais de arenitos e carbonatos.** Dissertação de mestrado, programa de pós-graduação em exploração petrolífera e mineral, Universidade Federal de Campina Grande, Campina Grande.

APOLINÁRIO, F.O. (2016). **Influência da saturação fluida nas propriedades elásticas de rochas carbonáticas.** Dissertação de mestrado, programa de pós-graduação em exploração petrolífera e mineral, Universidade Federal de Campina Grande, Campina Grande.

BIOT, M.A. (1956a). **Theory of propagation of elastic waves in a fluid saturated porous solid**, I. Low frequency range: J. Acoust. Soc. Am., 28, 168-178.

BIOT, M.A. (1956b). **Theory of propagation of elastic waves in a fluid saturated porous solid, II**. Higher frequency range: J. Acoust. Soc. Am., 28, 179-191.

BIOT, M.A. (1962)**. Mechanisms of deformation and acoustic propagation in porous media.** J. Appl. Phys., 33, 1482–1498.

BROWN, R.; KORRINGA, J. (1975). **On the dependence of the elastic properties of a porous rock on the compressibility of the pore fluid.** Geophysics, vol. 40, pp. 608-616.

GASSMANN, F. (1951). **Elastic waves through packing of spheres**. Geophysical Prospecting, pp. 673-685.

GRISCENCO, P. C. (2015). **Inversão de atributos sísmicos para caracterização e monitoramento de reservatórios.** Dissertação de Mestrado, Departamento de Astronomia, geofísica e ciências atmosféricas da terra. Usp, São Paulo.

SENGUPTA, M. (2000). **Integrating Rock Physics and Flow Simulation to Reduce Uncertainties in Seismic Reservoir Monitoring,** tese de doutorado, Departamento de Geofísica, Universidade de Stanford, Califórnia.

TROVÃO, A. A. F. (2015). **Análise de teorias de substituição de fluidos em afloramentos oriundos do Nordeste Brasileiro: uma abordagem petrofísica e ultrassônica.** Dissertação de mestrado, programa de pós-graduação em geofísica, Universidade Federal do Pará. Belém-PA.